Supporting information

Linear and nonlinear viscoelastic properties of segmented silicone-urea copolymers: influence of the hard segment structure

Guillaume Falco[a], Léo Simonin[b], Sandrine Pensec[b], Florent Dalmas[a], Jean-Marc Chenal[a], Laurent Bouteiller[b], Laurent Chazeau[a]

Table of contents

Characterization of the five silicone-urea copolymers by SEC and RMN:

(A)

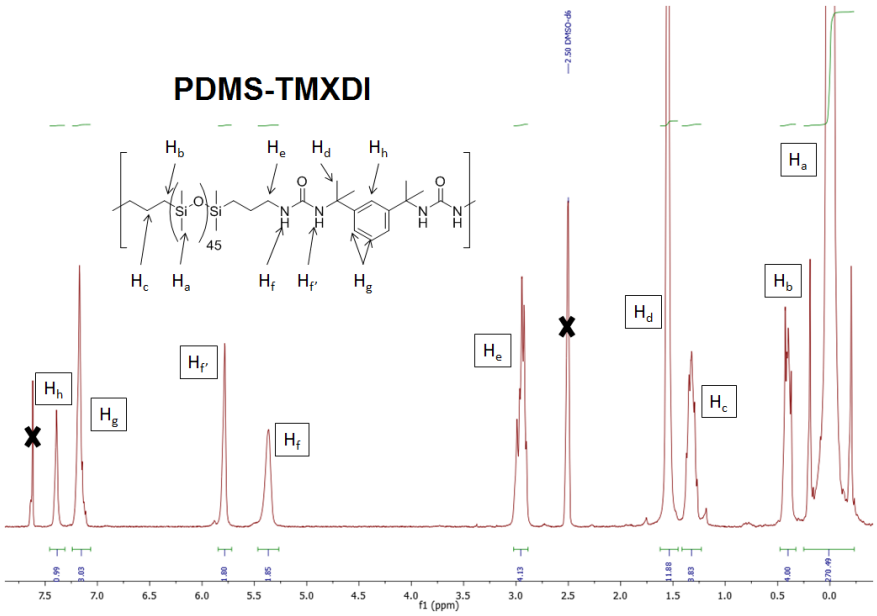

(B)

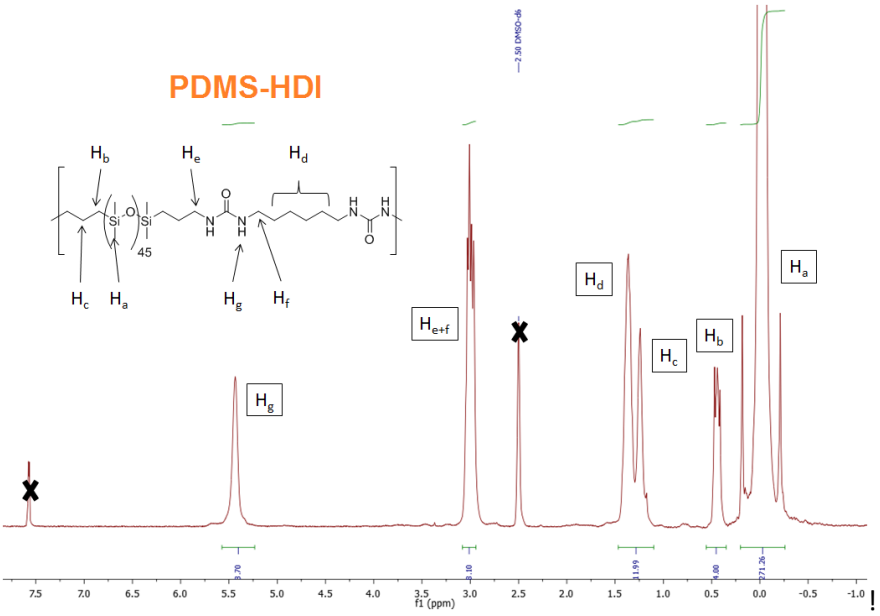

(C)

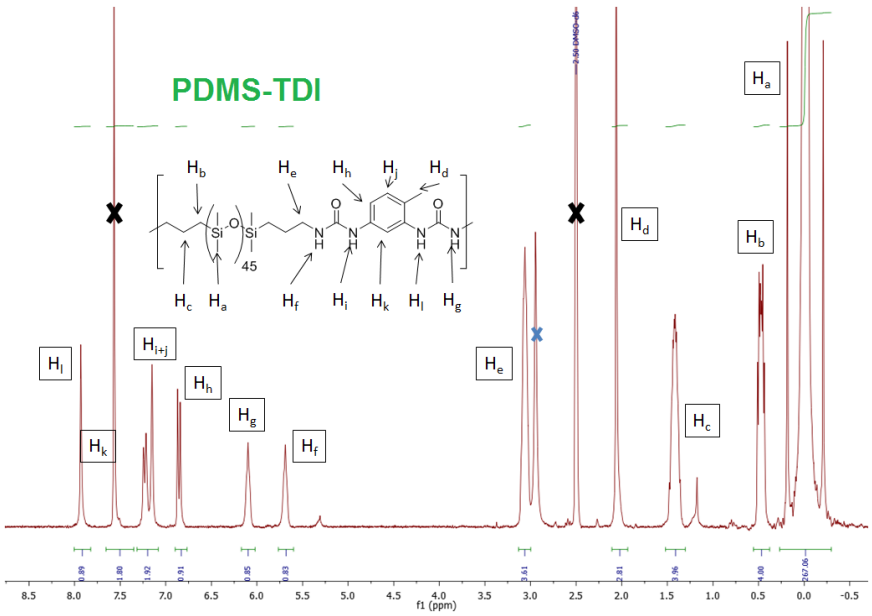
PDMS-TDI
Hb
He
Hh
Hj
Hd
45
Hc
Ha
Hf
Hi
Hk
Hl
Hg
Ha
Hd
Hb
Hl
Hi+j
Hh
Hg
Hf
Hk
He
Hc
f1 (ppm)

(D)

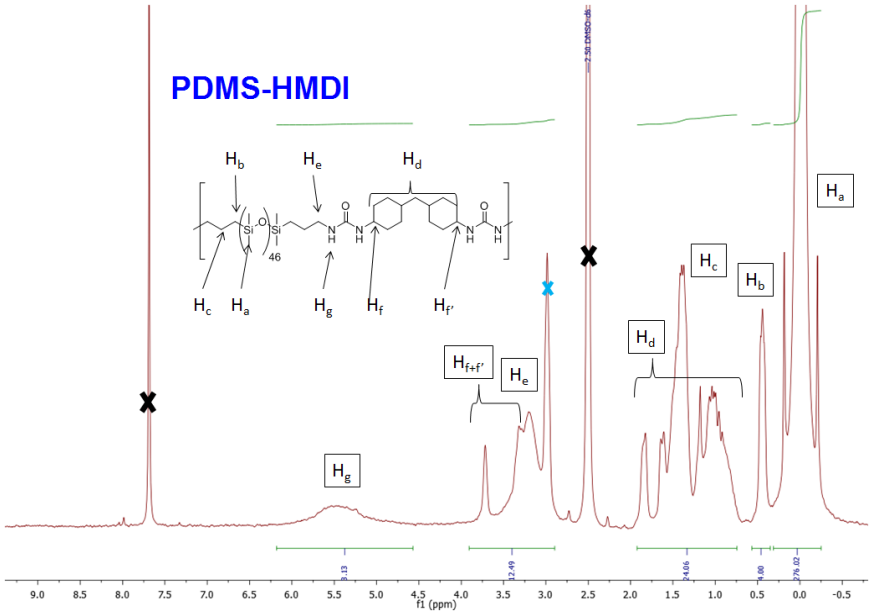
PDMS-HMDI
Hb
He
Hd
46
Hc
Ha
Hg
Hf
Hf'
Ha
Hc
Hb
Hd
Hf+f'
He
Hg
f1 (ppm)

(E)

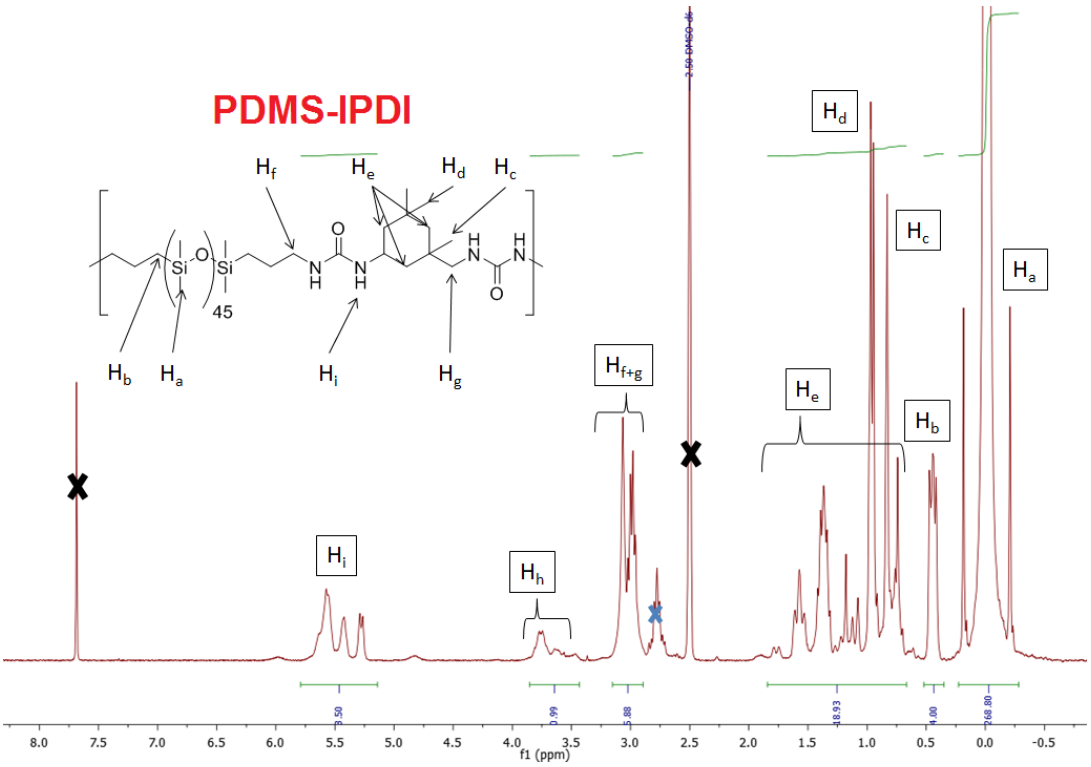

Figure S1: ^{1}H NMR spectra in $CDCl_3$/DMSO-d_6 of PDMS-TMXDI (A), PDMS-HDI (B), PDMS-TDI (C), PDMS-HMDI (D) and PDMS-IPDI (E). Black crosses represent NMR solvent ($CDCl_3$, DMSO d_6) and the blue cross represents residual water.

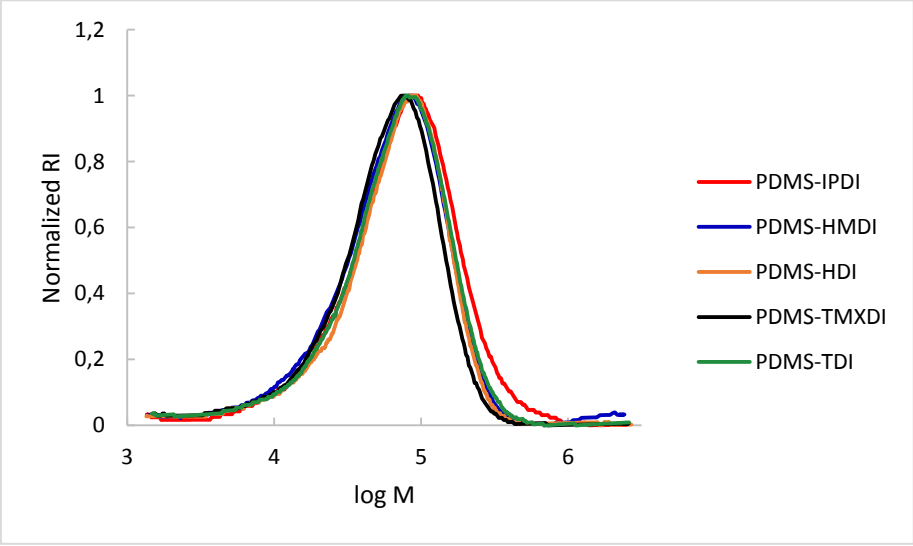

Figure S2: molar weight distribution from SEC for the five PDMS-urea segmented copolymers in THF.

Bisurea-HS models synthesis:

Bisurea-TMXDI was synthesized in a 50mL flask by addition of 2-ethylhexylamine (0.69g, 5.28mmol) on a solution of 1,3-bis(1-isocyanato-1-methylethyl)benzene (TMXDI, 0.6g, 2.41mmol) in 5mL dry dichloromethane. A precipitated was formed immediately. The reaction was followed by FT-IR spectroscopy to checked the disappearance of isocyanate peak (2273cm^{-1}). After 20h at room temperature, the product, which has precipitated, was filtrated. The white solid was then dried under vacuum (10^{-3} mbar) at 60°C for 1 day. Finally, 1.08g of bisurea-TMXDI was recovered with a yield of 89%.

1H NMR (300MHz, CDCl3/ d6-DMSO): δ (ppm)= 7.38 (s, Ar-*H*, 1H), 7.15 (m, Ar-*H*, 3H), 5.85 (s, N-*H*, 2H), 5.35 (m, N-*H*, 2H), 2.90 (m, NH-CH_2, 4H), 1.53 (s, C(CH_3)$_2$, 12H), 1.19 (m, C*H*(CH_2-CH$_3$)(CH_2)$_3$CH$_3$, 18H), 0.76 (m, CH_3, 12H)

Bisurea-HDI was synthesized in a 50mL flask by mixing 0.59g (3.46mmol) of hexamethylene diisocyanate and 1.00g (7.64mmol) of 2-ethylhexylamine in 10mL of dry dichloromethane. After 20h at room temperature, the product, which has precipitated, was filtrated. The white solid was then dried under vacuum (10^{-3} mbar) at 60°C for 1 day. Finally, 1.01g of bisurea-HDI was recovered with a yield of 68%.

1H NMR (300MHz, CDCl3/ d6-DMSO): δ (ppm)= 5.21 (s, N-*H*, 2H), 5.11 (s, N-*H*, 2H), 2.86 (m, CH_2NH, 8H), 1.10 (m, CH$_2$(CH_2)$_4$CH$_2$, C*H*(CH_2-CH$_3$)(CH_2)$_3$CH$_3$, 26H), 0.66 (m, CH_3, 12H)

Intensity line profiles from AFM phase images of of PDMS-TMXDI, PDMS-HDI and PDMS-TDI

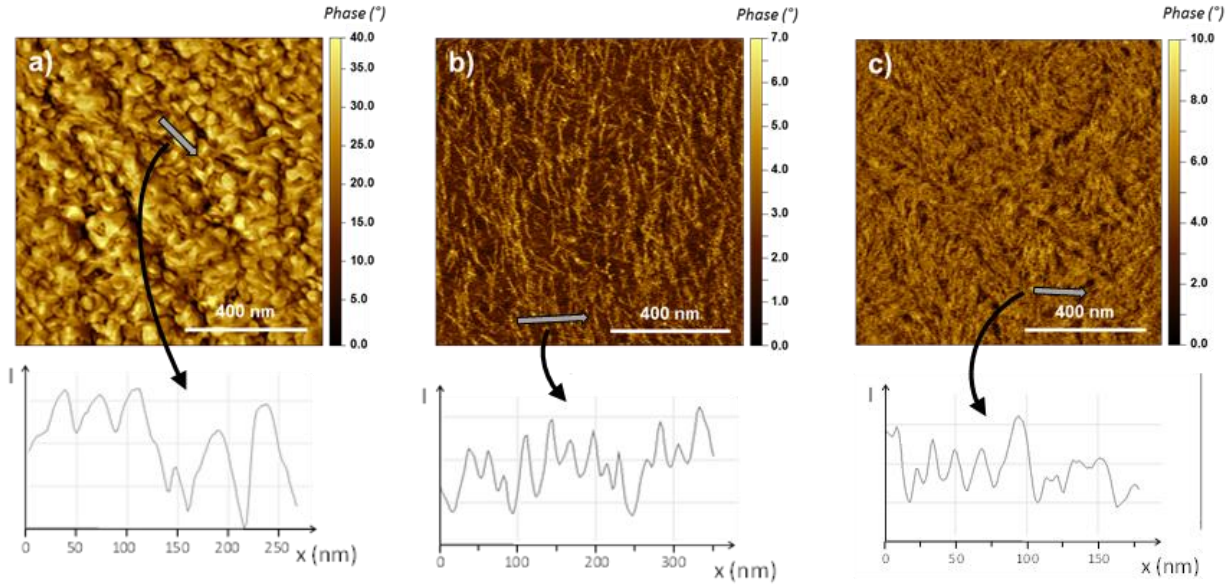

Figure S3: Tapping-mode AFM phase images at room temperature and intensity lines profile of a) PDMS-TMXDI, b) PDMS-HDI, c) PDMS-TDI. Intensity line profiles along indicated arrows on higher magnification images are shown in order to highlight the nanostructure characteristic size.

Note that Fourier Transform of the AFM images does not provide additional information and less conclusive.

Experimental and theoretical distance between hard segment centers in a copolymer chain:

Given the SAXS peaks at q ca. 1.2 - 1.5 nm^{-1} of the five segmented silicon-urea copolymers, experimental distance between hard segment centers on a same polymer chain ($D_{Experimental}$) can be deduced following the formula : $D_{Experimental} = 2\pi/q$ and compared to the theoretical distance ($D_{theoretical}$) where :

$D_{theoretical} = L_{HS} + L_{PDMS}$

with L_{HS} is the theoretical length of the hard segment, calculated from the length and the angle of each bond.

L_{PDMS} is the theoretical length of the PDMS soft segment, calculated within the assumption of a Gaussian behavior. From Fetters Review[1], which claim that $\langle R_0^2 \rangle / M$ is equal to 0,00457 $nm^2.g.mol^{-1}$, given a molar weight of 3250 $g.mol^{-1}$ for the PDMS block, L_{PDMS} is found equal to 3.7 nm

All the deduced values are reported in the table below:

	PDMS-TMXDI	PDMS-HDI	PDMS-TDI	PDMS-HMDI	PDMS-IPDI
q (nm^{-1})	1.24	1.23	1.48	1.23	1.36
$D_{Experimental}$ (nm)	5.1	5.1	4.2	5.1	4.6
L_{HS} (nm)	1.2	1.4	1.0	1.5	1.1
$D_{theoretical}$ (nm)	4,9	5,1	4,7	5,2	4,8

In all systems, $D_{theoretical}$ is remarkably close to the experimental value. Moreover, $D_{Experimental}$ varies like L_{HS}

References:

[1] L.J. Fetters, D.J. Lohse, D. Richter, T.A. Witten, A. Zirkel, Connection between polymer molecular weight, density, chain dimensions, and melt viscoelastic properties, Macromolecules. 27 (1994) 4639–4647.

I(q) fitting of the SAXS data to estimate a characteristic distance in PDMS HDI and PDMS TDI :

Table 1: Recapitulative table with the characteristic distances revealed by AFM and SAXS for PDMS-TMXDI, PDMS-HDI and PDMS-TDI

	PDMS-TMXDI	PDMS-HDI	PDMS-TDI
D_{AFM} (nm)	40-50	20-30	15-20
D_{SAXS} (nm)	-	34	22

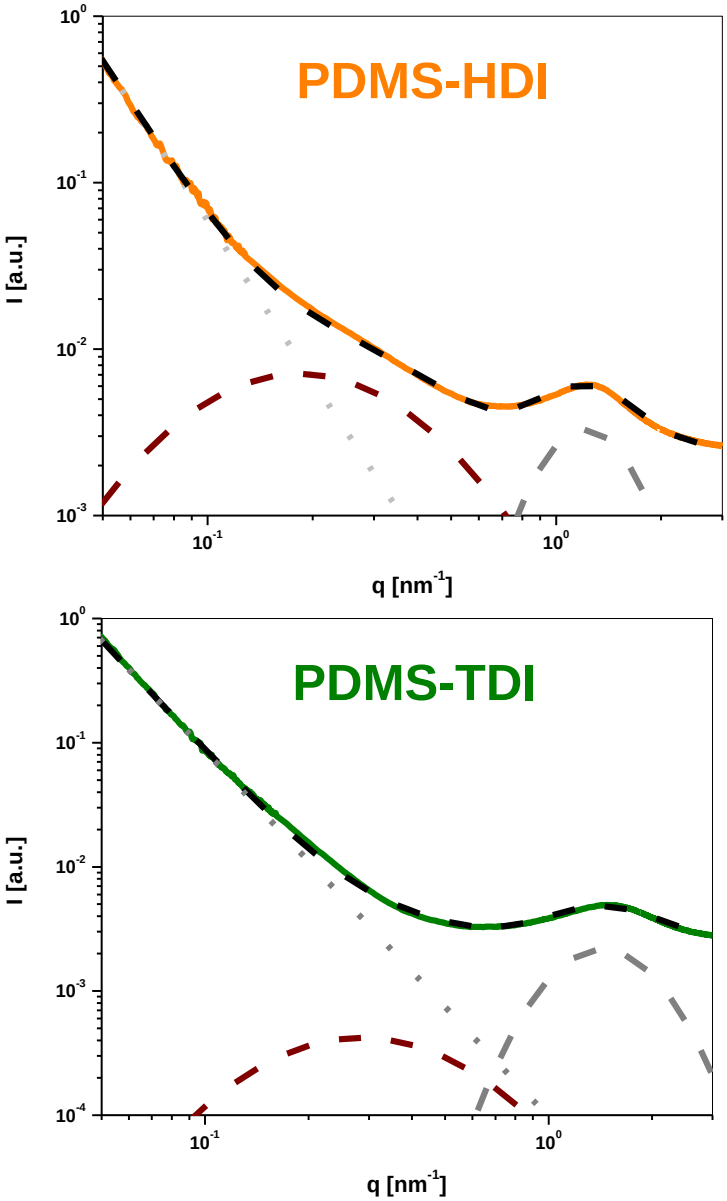

	linear slope fit ($y=a*e^{b}$) (dotted gray line)		Additional peak fitted by the log normal function (dash brown line)			First peak fitted by the log normal function (dash gray line)		
	a	b	A	w	x_c	A	w	x_c
PDMS-HDI	$3.90*10^{-5}$	-3.180	$2.85*10^{-3}$	0.689	0.295	$3.02*10^{-3}$	0.290	1.320
PDMS-TDI	$9.65*10^{-5}$	-2.950	$2.45*10^{-4}$	0.658	0.440	$2.80*10^{-3}$	0.342	1.610

Figure S4: SAXS/USAXS curves, fits and fitting parameters for PDMS-HDI and PDMS-TDI. The addition of the three fitted curves is represented in black dotted line and include an y_0 constant of 2.6 $*10^{-3}$ corresponding to the continuous background. Given the very weak shoulder in the I(q) curve, a simple log normal function has been chosen to deduce the intermediate distance. Even though a characteristic distance can be deduced in AFM for PDMS-TMXDI, it is not surprising to not evidence it by SAXS as it should be in the range of the large I(q) increase (q around 0.1 nm^{-1}).

DSC of the hard segments models (i.e. bisurea-TMXDI and bisurea-HDI)

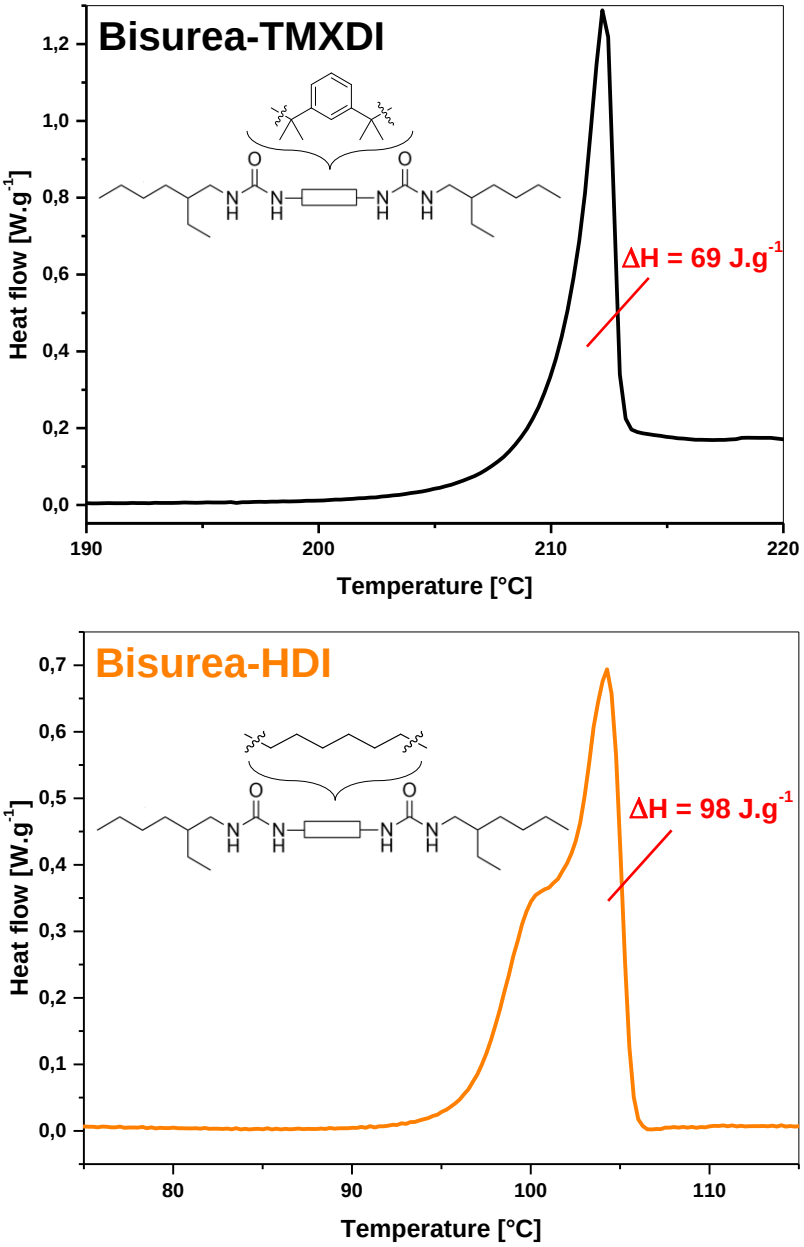

Figure S5: DSC heating scan at 2°C.min^{-1} (under N_2 flux) showing the melting enthalpy and the structure (insert) of bisurea-TMXDI and bisurea-HDI (models for the hard segments).

DSC data of the five segmented copolymers

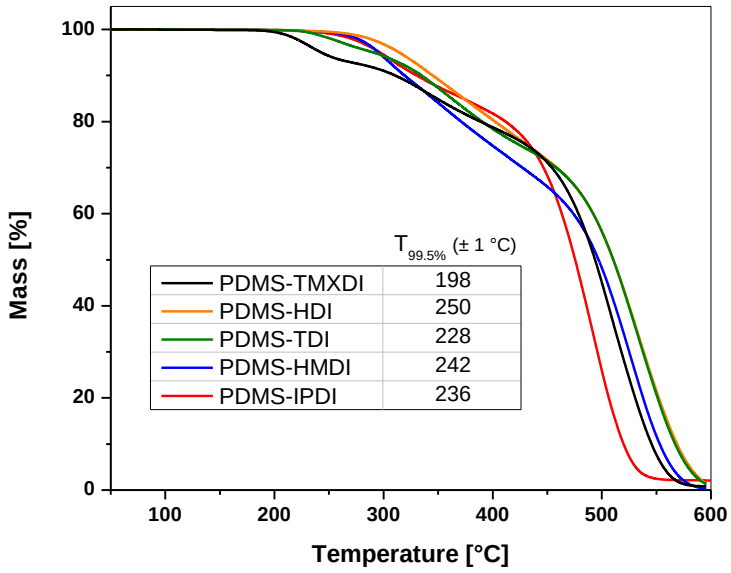

Figure S6: Non-isothermal thermogravimetric measurements (10 °C.min^{-1}) under N_2 atmosphere of the five segmented silicone-urea copolymers. The starting degradation temperature ($T_{99.5\%}$) is reported in the table in insert.

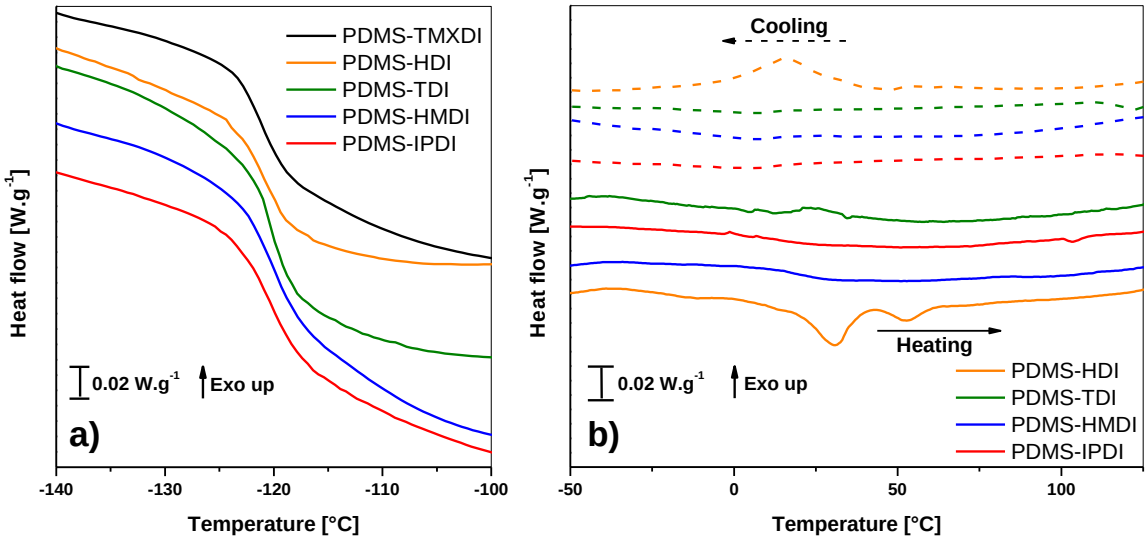

Figure S7: Raw non-isothermal DSC measurements (10 °C.min^{-1}) of the segmented silicone-urea copolymers. a) glass transition temperature range. b) DSC data from -50 °C to 125 °C highlighting the absence of exothermic peak for PDMS-TDI, PDMS-HMDI, PDMS-IPDI; the PDMS-HDI thermograms at 2°C.min^{-1} has been added for comparison ($\Delta H = \pm 2.4$ J.g^{-1}).

SAXS and WAXS data as a function of the temperature for PDMS-HMDI and PDMS-IPDI

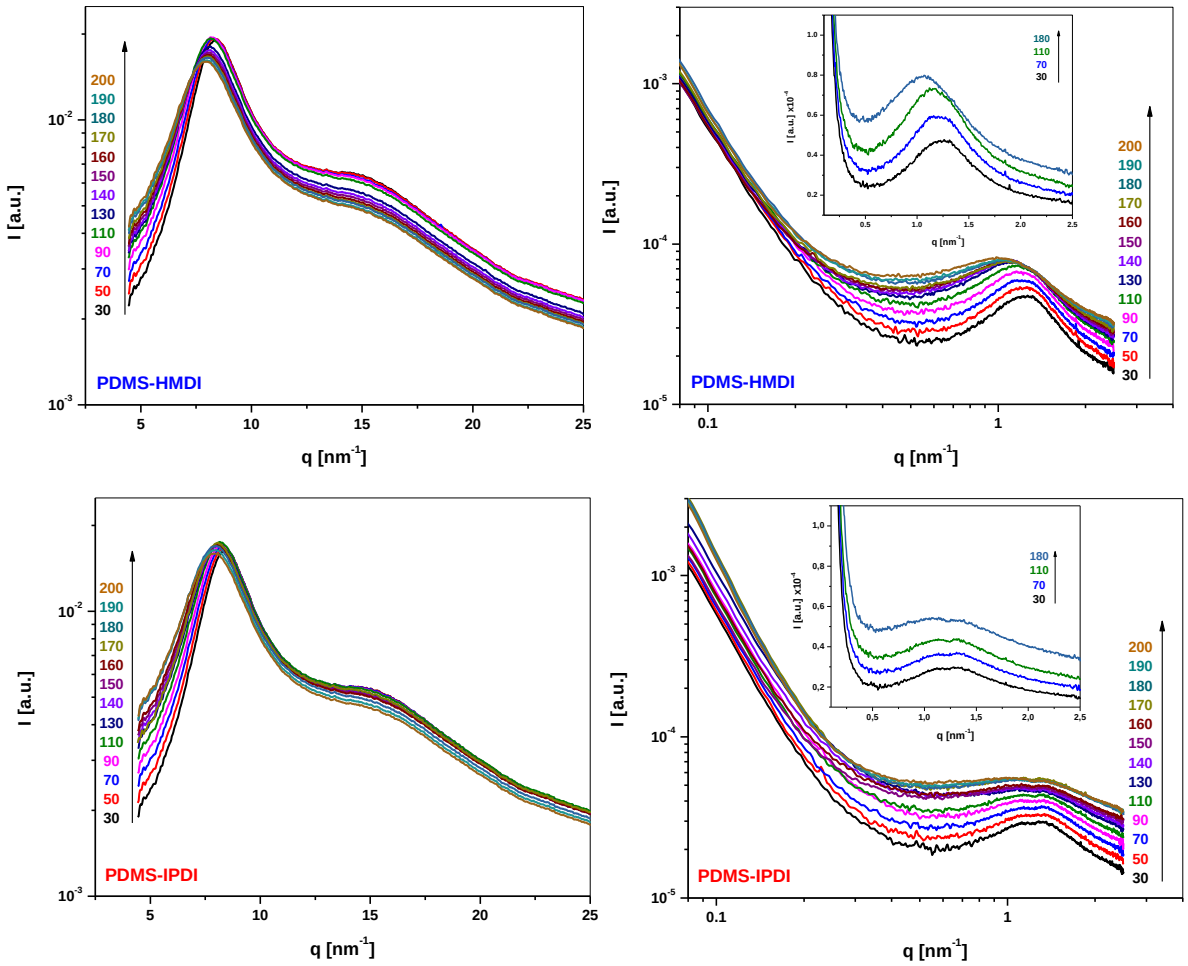

Figure S8: (left) WAXS and (right) SAXS spectra obtained for PDMS-HMDI and PDMS-IPDI at different temperatures ranging from 30°C to 200°C.

Explanation of the evolution with temperature of the scattered intensity in the [0.3 nm^{-1}; 3 nm^{-1}] domain:

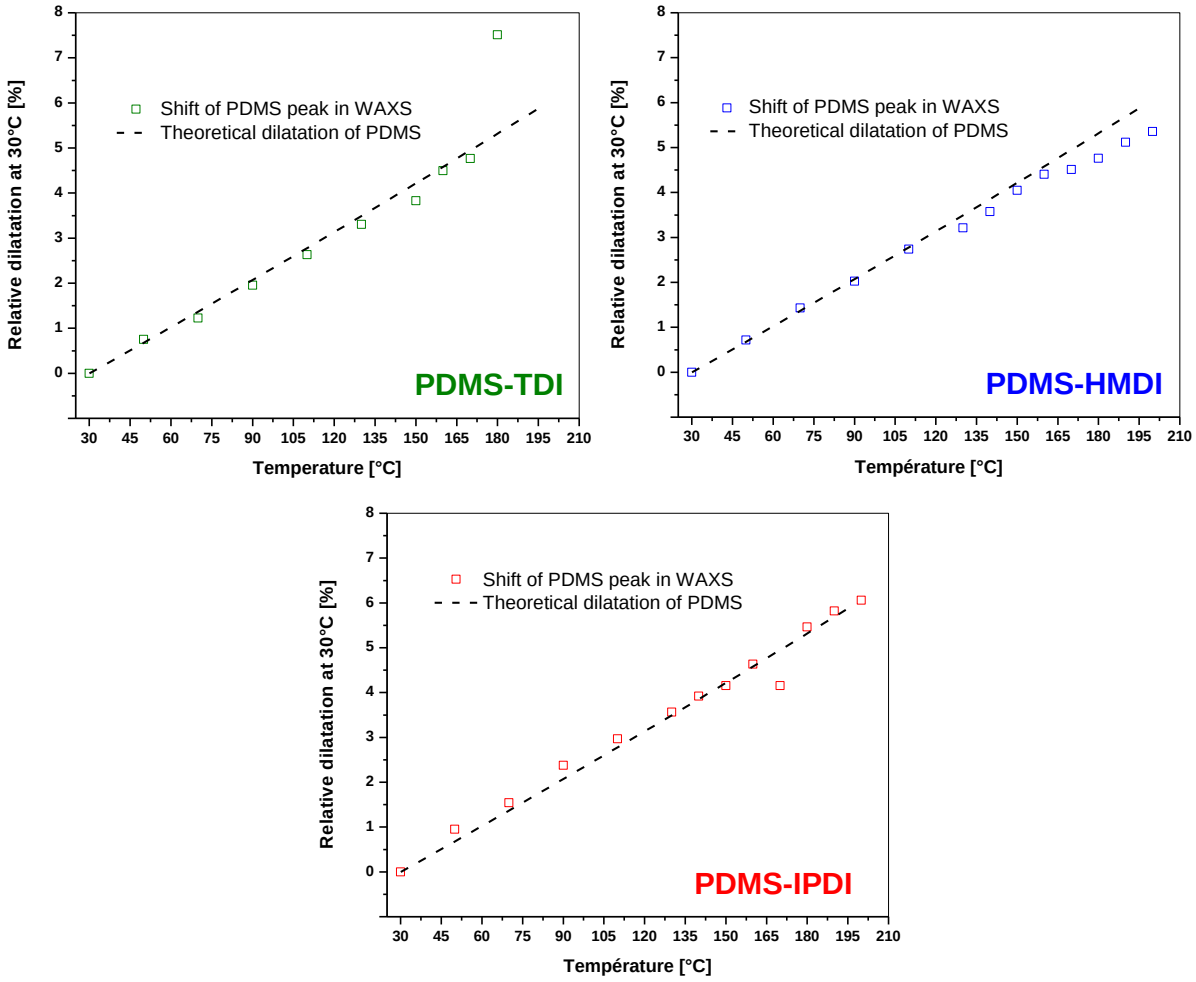

Figure S9: Relative thermal dilatation (at 30°C) of the PDMS-TDI, PDMS-HMDI and PDMS-IPDI evaluated from the shift of the PDMS peak at around 8 nm^{-1} in WAXS. The theoretical dilatation of the PDMS was also plot (in black line) to show the perfect fit with the dilatation of the samples.

In order to better understand the variation with temperature of the peak previously ascribed to the distance between the hard segment phase, the q^{-m} dependence have been subtracted from the scattered intensity (**Figure S10**). The intensity variation of this peak with the temperature increase is very similar for the three materials. It can be ascribed to the variation of the scattering contrast, this one being equal to the square of the difference between the scattering length density of HS (ρ_{HS}) and SS (ρ_{SS}) domains. For instance, at room temperature, the values of ρ_{HS} and ρ_{SS} for PDMS-TDI sample are respectively around 9,4 10^{10} cm^{-2} and ρ_{SS} 8,2 10^{10} cm^{-2}. According to Figure S9, SS domain governs the thermal dilatation and consequently the ρ_{SS} variation with temperature is more important than the one of HS domains. ρ_{SS} decreases down to 6,9 10^{10} cm^{-2} at 170°C: assuming that ρ_{HS} remains constant, this variation leads to a phase contrast increase by a factor largely above 2, consistent with the observed increase in the scattered intensity (by a factor 2) with the temperature.

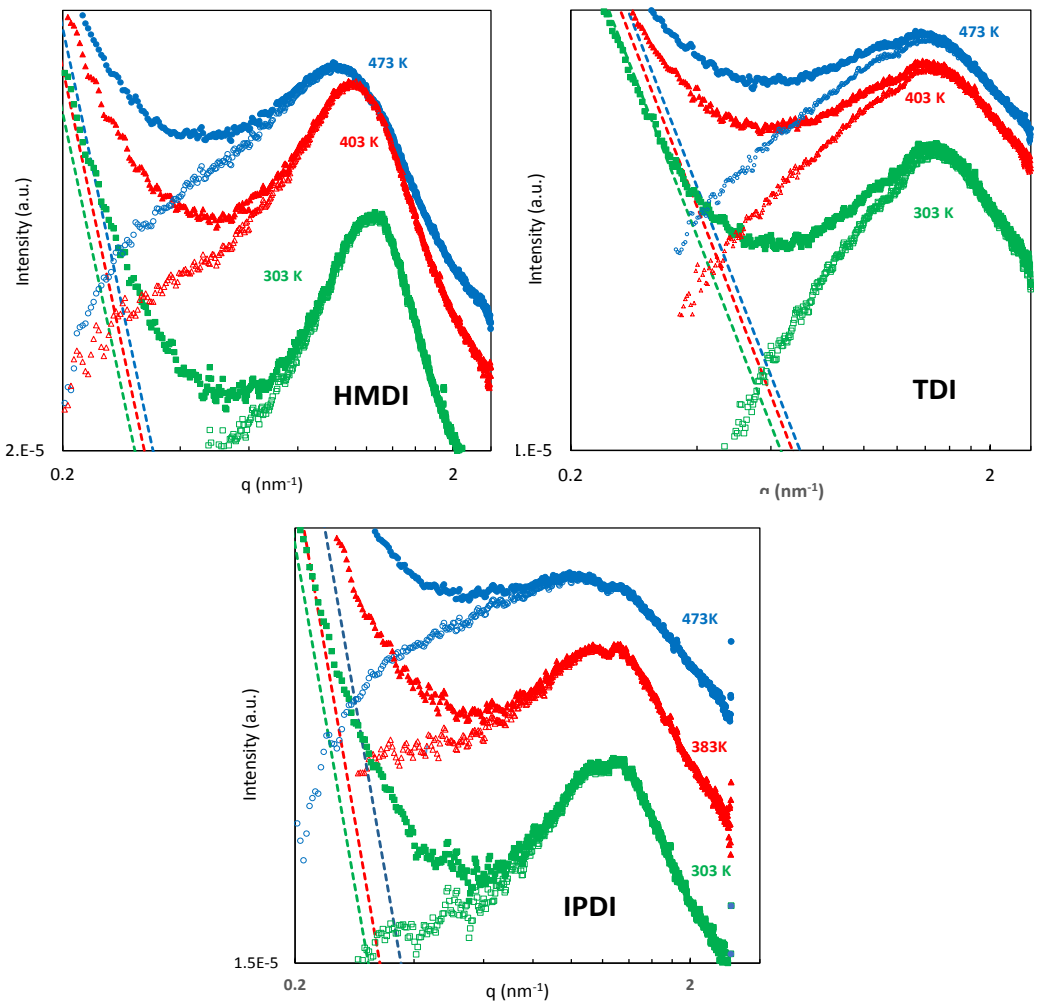

Figure S10: SAXS/USAXS curves obtained at 303 K, 383 K and 473 K for PDMS-HMDI, PDMS-TDI and PDMS-IPDI in the [0.2 nm^{-1}; 2.5 nm^{-1}] q domain. The fitted q^{-m} variation at lower q is represented in dotted lines and was subtracted from the experimental data (empty symbols).

Isothermal DMA curves at 160°C:

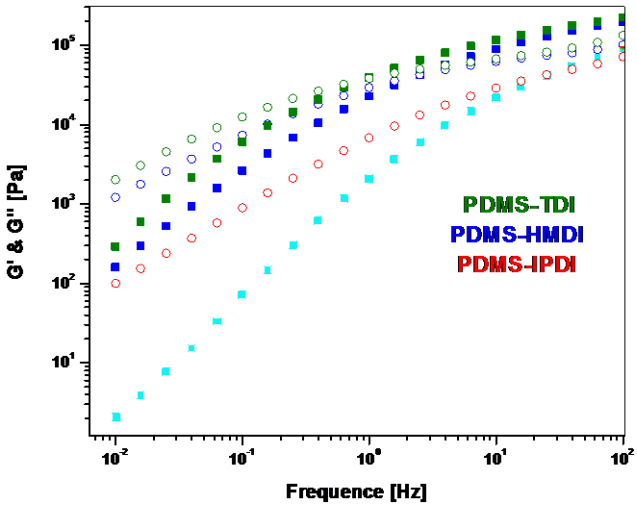

Figure S11: G’ (full square) and G’’ (open circle) obtain by a frequency sweep of PDMS-TDI, PDMS-HMDI and PDMS-IPDI at 160 °C.

Cole-Cole representation (G'' vs. G') *to check the TTS validity:*

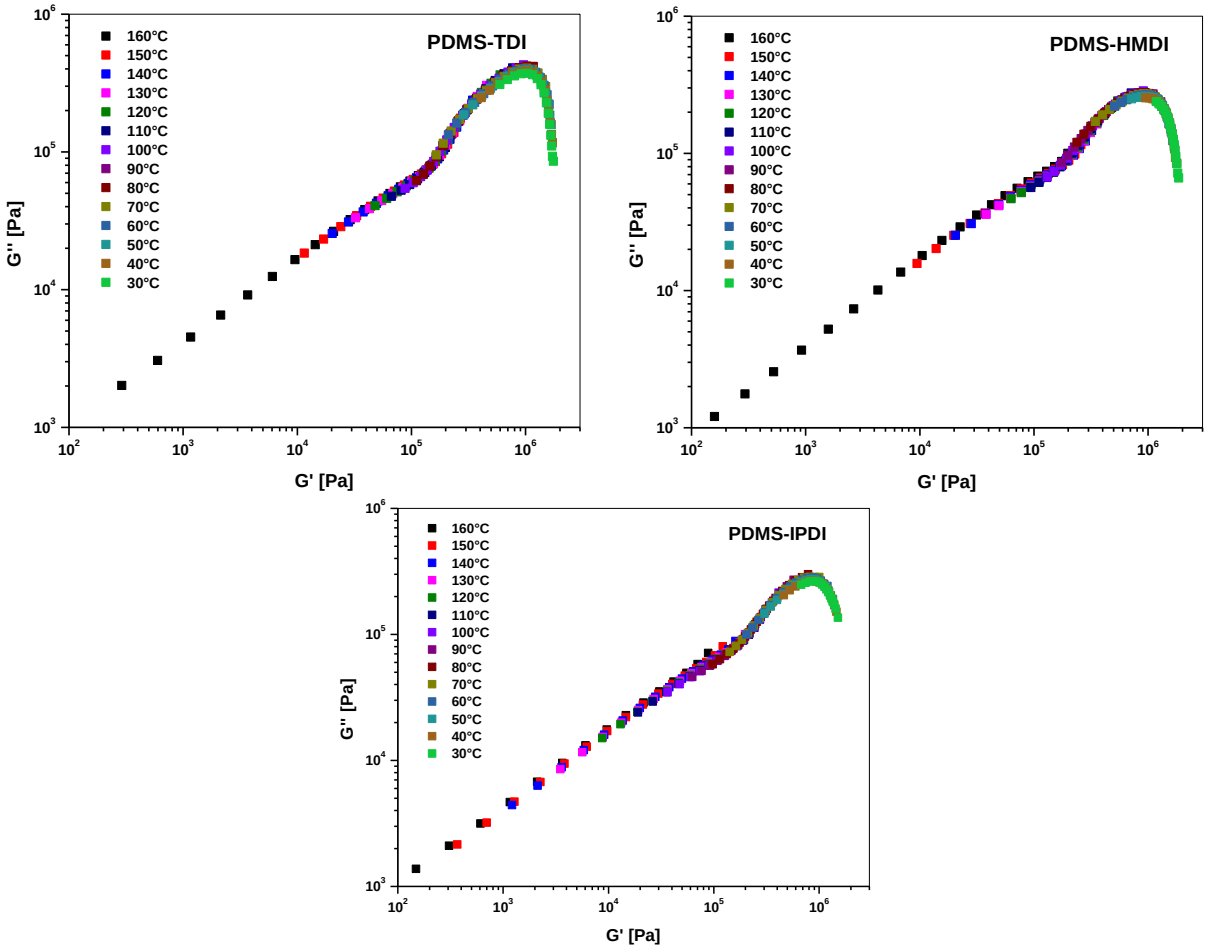

Figure S12: Cole-Cole representation (G'' vs. G') of PDMS-TDI, PDMS-HMDI and PDMS-IPDI using the frequency sweeps data of rheology measurements. The three copolymers highlight an optimal superposition over the chosen temperature range (30°C to 160°C).

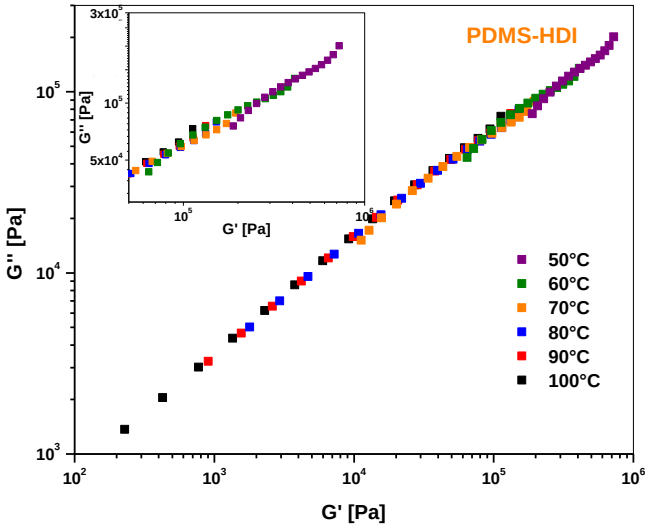

Figure S13: Cole-Cole representation (G" vs. G') of PDMS-HDI using the frequency sweeps data of rheology measurements highlighting the poor superposition below 60°C.

FTIR measurements as a function of the temperature:

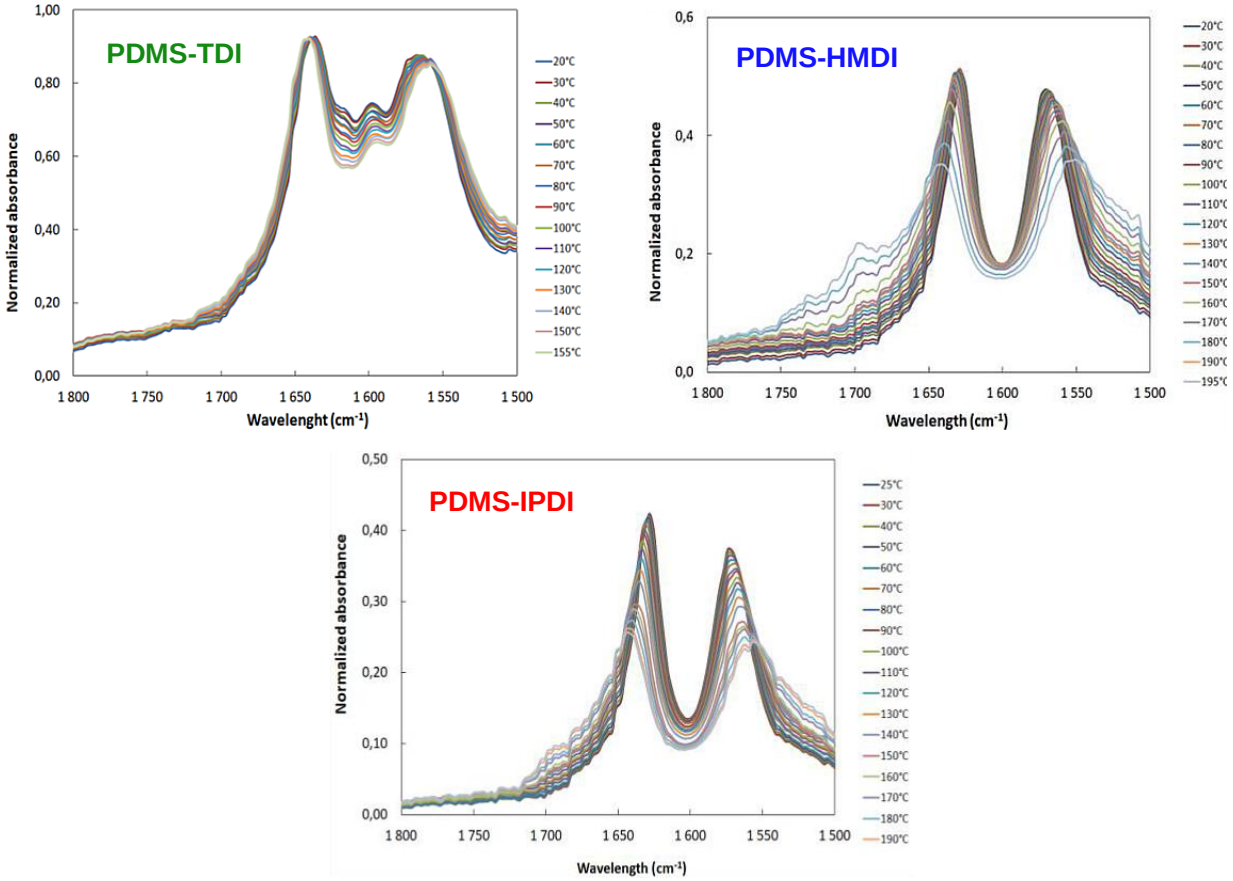

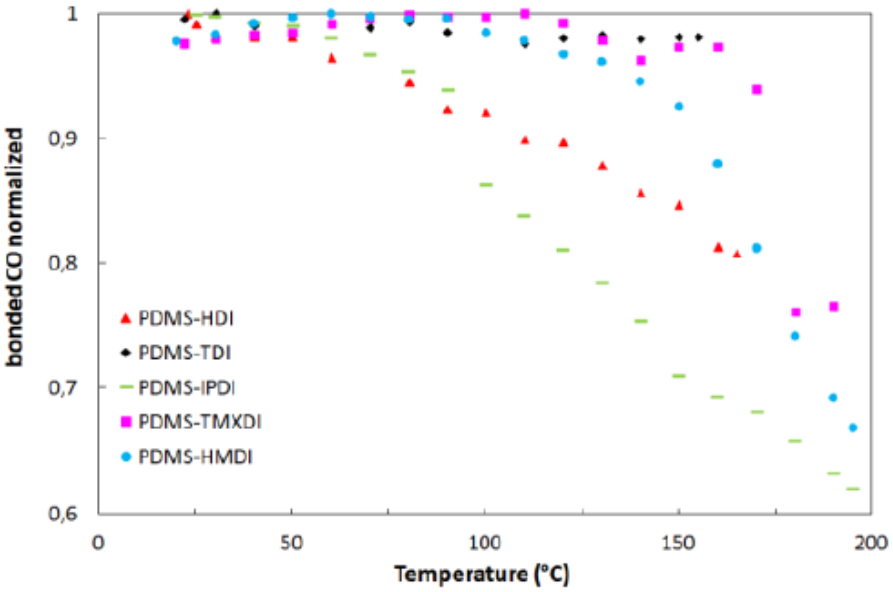

Figure S14: Normalized FT-IR spectra (at 2950cm^{-1}) of PDMS-TDI, PDMS-HMDI and PDMS-IPDI in the 1500-1800 cm^{-1} region showing the variation of the fraction of the associated (~ 1650 cm^{-1}) and non-associated (~ 1700 cm^{-1}) CO-NH bonds with temperature. Bottom: variation of the relative fraction of associated CO groups with temperature, deduced from FT-IR spectra.

Crack healing behavior :

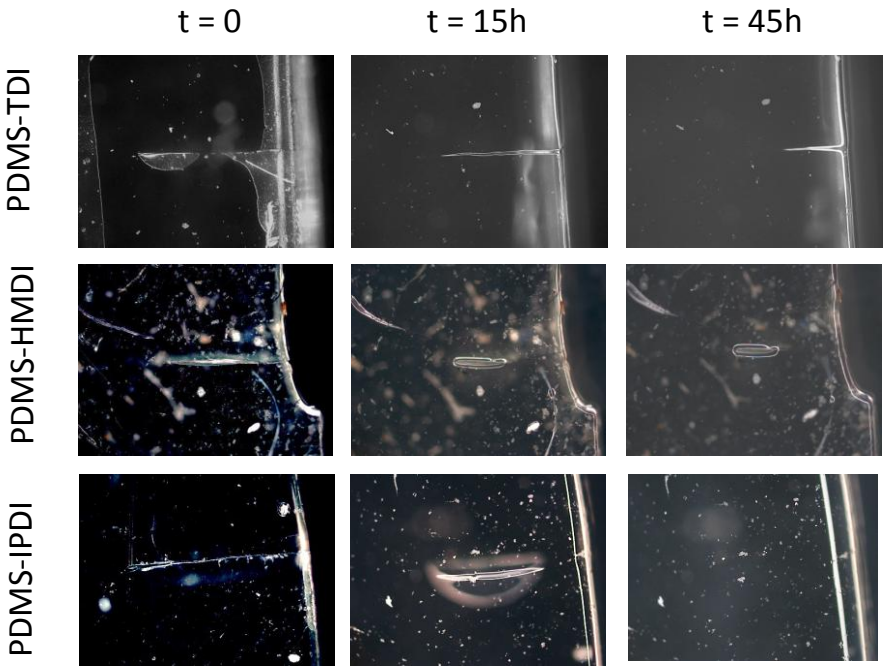

Figure S15: Optical micrograph showing self-healing properties of PDMS-TDI, PDMS-HMDI and PDMS-IPDI material at 50°C.

Extrapolation of τ_{term} at ambient temperature:

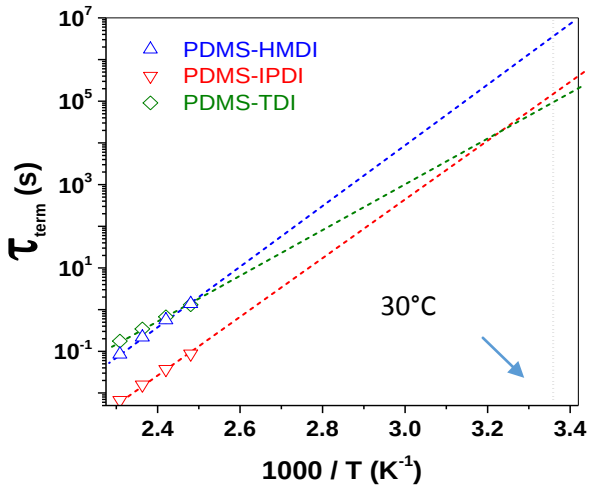

Figure S16: τ_{term} deduced from the isothermal curves as a function of 1000/T for PDMS-TDI, PDMS-HMDI and PDMS-IPDI, with an exponential extrapolation at low temperature.